

# The Relationship between the Grid Size and the Coefficient of Nonlinear Lateral Eddy Viscosity in Numerical Ocean Circulation Models

ROBERT L. HANEY AND JULIAN M. WRIGHT, JR.

*Department of Meteorology, Naval Postgraduate School, Monterey, California 93940*

Received March 13, 1975

When a constant coefficient of lateral eddy viscosity  $\nu_0$  is used in ocean circulation models, a false computational space oscillation is generated in the western boundary region if  $\nu_0$  is smaller than a critical value. The use of a nonlinear eddy viscosity coefficient based upon two-dimensional turbulence theory is shown to permit the use of an eddy viscosity which, away from the western boundary region, is at least an order of magnitude smaller than the above critical value.

## 1. INTRODUCTION

In the linear theory of the steady wind driven ocean circulation [1], the solution for the mass transport stream function has a westward intensification and an associated western boundary current of width

$$L_w = (2\pi/\sqrt{3})(\nu_0/\beta)^{1/3} \quad (1)$$

where  $\nu_0$  is the constant coefficient of lateral eddy viscosity and  $\beta = (2\Omega \cos \varphi)/a$ , where  $\Omega$  is the earth's rotation rate,  $\varphi$  is latitude, and  $a$  is the radius of the earth. This westward intensification and frictional boundary layer also exists in more realistic numerical models of the world ocean [2, 4] and it places a lower limit on the value of  $\nu_0$  that can be used with a given grid size. To be exact, Takano [3] showed that if  $\nu_0$  is sufficiently small such that

$$L_w \leq \Delta x/0.76, \quad (2)$$

where  $\Delta x$  is the east-west grid size, a false computational space oscillation appears in the numerical solution. On the other hand, in a numerical general circulation model with  $\Delta x \sim 300$  km, if  $\nu_0$  is made large enough to prevent the false space oscillation, the open ocean solution is too viscous. Takano [3] further showed that the selective use of a slightly uncentered (upstream) finite difference approximation to the beta-term in the vorticity equation suppresses the false oscillation

and thereby allows the use of a value of  $\nu_0$  which is 50 % smaller than the minimum which satisfies (2).

However, if one is interested in large-scale time-dependent motion in the open ocean (as in the North Pacific Experiment), then the above technique is not very satisfactory because the upstream differencing results in excessive damping of the transient motion. In addition, a realistic value of the lateral eddy viscosity in the open ocean which parameterizes the statistical effects of all motions on a scale smaller than the grid size is at least an order of magnitude smaller than that allowed by (2) [5, 6]. Indeed, there are open ocean motions which, in fact, produce a negative eddy viscosity in the horizontal plane [7, 8] and it is hoped that by sufficiently reducing the *sub-grid-scale* eddy viscosity, more energetic and realistic *grid-scale* motions will be allowed to develop [8]. In order to do this, a more satisfactory approach from both a computational and a physical point of view is to use nonlinear eddy viscosity coefficients [9–11]. Nonlinear eddy viscosity coefficients are increasingly sensitive to the spatial scale of the motion and therefore will be relatively small in the interior where the scales of motion are comparatively large and will be relatively large in the western boundary region where the scales are comparatively small. The condition (2) will be satisfied locally in the western boundary region, thereby preventing the false computational oscillation, while the interior ocean will enjoy a generally reduced and more realistic level of lateral eddy viscosity. Nonlinear lateral eddy viscosities have been used in ocean circulation models before [12, 13], but not for this express purpose.

## 2. NONLINEAR EDDY VISCOSITY

In a numerical model, the frictional force which arises due to lateral eddy viscosity parameterizes the convergence of horizontal momentum by oceanic eddy motions which are too small to be explicitly resolved by the grid. Since these motions are to a great extent geostrophic and quasihorizontal, it is appropriate to use eddy viscosity coefficients which are based on the theories of two-dimensional turbulence [11, 14, 15]. Using the conservation laws of energy and square vorticity (enstrophy) which hold for two-dimensional turbulence, Kraichnan [14] and Leith [15] proved the existence of an inertial range in which the kinetic energy spectrum  $E(k)$  has a  $-3$  power law

$$E(k) = \alpha_1 \eta^{2/3} k^{-3}, \quad (3)$$

where  $\alpha_1$  is a proportionality constant,  $\eta$  is the constant enstrophy cascade rate, and  $k$  is the wavenumber in the inertial range. It should be noted that the analogy between this  $-3$  power law for 2-D turbulence and the familiar  $-5/3$  power law

for 3-D turbulence is weak. The  $-3$  power law is only an asymptotic state which may or may not be attained in a finite amount of time depending on the initial state. Under the additional assumption that the eddy viscosity coefficient  $\nu$  is a function of  $\eta$  and  $k$  alone, one obtains by dimensional considerations

$$\nu = \alpha_2 \eta^{1/3} k^{-2}, \quad (4)$$

where  $\alpha_2$  is a nondimensional constant. This same relationship was derived by Bye [11] for two-dimensional motion in a homogeneous ocean in which the dissipation occurs in a bottom-friction layer. Following Smagorinsky [9] and Leith [10], the viscosity coefficient is made nonlinear by substituting into (4) the local value of the enstrophy dissipation rate, which is

$$\eta = \nu \nabla \zeta \cdot \nabla \zeta, \quad (5)$$

where  $\zeta$  is the relative vorticity and  $\nabla$  is the horizontal del-operator. The resulting eddy viscosity coefficient becomes

$$\nu = \alpha_2^{3/2} (\nabla \zeta \cdot \nabla \zeta)^{1/2} k^{-3}. \quad (6)$$

If one now assumes that the space truncation wavenumber  $k = 2\pi/\Delta x$  lies within the  $-3$  power inertial range [10], then according to (6),  $\nu$  is proportional to the magnitude of the gradient of relative vorticity computed on the grid. This is the basis for the form of lateral eddy viscosity used below.

### 3. RESULTS OF THE NUMERICAL EXPERIMENTS

The goal of these numerical experiments is to see whether the use of a nonlinear eddy viscosity coefficient can permit a generally low and realistic value of  $\nu$  to be used in the ocean interior and at the same time can suppress the computational space oscillation which would be generated in the western boundary region if the same low value were used uniformly over the entire basin. For this purpose the eddy viscosity coefficient is written

$$\nu = \nu_0 (1 + \gamma |\nabla \zeta| (\Delta x)^3), \quad (7)$$

where  $\nu_0$  and  $\gamma$  are constants. The quantity  $\nu_0$  essentially represents the minimum value of the eddy viscosity while  $\gamma$  determines the variation of  $\nu$  between the open ocean, where the vorticity gradient is smallest, and the western boundary region, where it is largest.

The above nonlinear eddy viscosity is applied to a barotropic model of the wind driven ocean circulation in a closed rectangular basin on a beta-plane.

Assuming the current is nondivergent and independent of depth, the resulting circulation is governed by the vorticity equation

$$\begin{aligned} \frac{\partial \zeta}{\partial t} = & -v\beta + \frac{\partial}{\partial x} \left( -\frac{\partial}{\partial x} (uv) - \frac{\partial}{\partial y} (vv) + F_y + \tau_y/\rho D \right) \\ & - \frac{\partial}{\partial y} \left( -\frac{\partial}{\partial x} (uu) - \frac{\partial}{\partial y} (vu) + F_x + \tau_x/\rho D \right), \end{aligned} \quad (8)$$

where  $u$  and  $v$  are the velocity components in the  $x$  and  $y$  directions which point eastward and northward, respectively. In (8),  $F_x$  and  $F_y$  are the  $x$  and  $y$  components of the friction force due to lateral eddy viscosity, and are given by

$$F_x = \nabla \cdot (\nu \nabla u), \quad F_y = \nabla \cdot (\nu \nabla v). \quad (9)$$

The quantity  $(\tau_x, \tau_y)$  is the surface wind stress,  $\rho$  is the (constant) density, and  $D$  is the (constant) depth. Bottom stress is neglected. Since the velocity is assumed nondivergent, it can be defined by a stream function  $\psi$ ,

$$v = \partial\psi/\partial x, \quad u = -\partial\psi/\partial y, \quad (10)$$

and upon substituting (10) into (8) a single equation in  $\psi$  is obtained. The boundary conditions of zero velocity at the lateral boundaries of the basin are expressed by setting the stream function and its normal derivative to zero,

$$\psi = \partial\psi/\partial n = 0, \quad \text{on boundaries.} \quad (11)$$

Numerical integrations out to 200 days were performed using a  $33 \times 17$  array of points with a constant grid interval  $d = \Delta x = \Delta y = 300$  km. Centered finite differences in space and time were used everywhere except in the lateral eddy viscosity term where a forward timestep was used. A Matsuno timestep [16] was used every 50 timesteps to prevent solution separation. Details of the numerical methods are in the appendix. Additional details of the numerical methods and results of tests with nonlinear eddy viscosity coefficients based on three-dimensional turbulence are given in Wright [20].

The circulation was forced by a steady wind stress curl which was a prescribed function of  $y$  alone,

$$\frac{\partial \tau_y}{\partial x} - \frac{\partial \tau_x}{\partial y} = -\frac{T\pi}{B} \sin\left(\frac{\pi y}{B}\right), \quad (12)$$

where  $T = 1 \text{ dyn cm}^{-2}$  and  $B = 4800 \text{ km}$  is the north-south extent of the basin.

Experiments were performed using two different values of  $\nu_0$ ; a moderate value  $\nu_M = 0.96 \times 10^8 \text{ cm}^2 \text{ sec}^{-1}$  for which the western boundary current width  $L_w = \Delta x$ , and a smaller value  $\nu_S = \nu_M/8$  for which  $L_w = \Delta x/2$ . Figure 1a shows the familiar steady state analytic solution obtained by Munk [1] using the eddy viscosity coefficient  $\nu_M$ .

Figure 1b shows the numerical solution at 200 days obtained on the 300 km grid using the constant eddy viscosity coefficient  $\nu_M$ . As predicted by the criterion of Takano (2), a very prominent computational space oscillation extends eastward from the western boundary because of the failure of the grid to properly resolve the western boundary current. In addition, the stream function is falsely amplified by a factor of almost 2 in the western boundary region. Figure 1c shows the numerical solution obtained on the same 300 km grid using the nonlinear eddy viscosity (7) with  $\nu_0 = \nu_M$  and  $\gamma = 0.55 \times 10^{-8} \text{ sec cm}^{-2}$ . It is clear that the false computational space oscillation and solution amplification are almost completely suppressed. The actual values of  $\nu$  computed at the grid points (not shown) vary from  $0.98 \times 10^8 \text{ cm}^2 \text{ sec}^{-1}$  throughout most of the open ocean to about  $5.5 \times 10^8 \text{ cm}^2 \text{ sec}^{-1}$  in the western boundary region.

Figure 2 shows the results of the more extreme case in which  $\nu_0$  is reduced by a factor of 8 over the previous case. When a constant viscosity is used (a), the solution is completely dominated and destroyed by a large-amplitude space oscillation which fills the entire basin. When nonlinear viscosity is used, and  $\gamma$  is moderately large (b), the false space oscillation is greatly suppressed and the western boundary solution is quite similar to Fig. 1a and therefore is as realistic as one can expect to obtain with a 300 km grid. When  $\gamma$  is increased by an order of magnitude (c), the false oscillation is completely suppressed; however, the western boundary current becomes broader and since its transport changes very little the current also becomes weaker. In both Figs. 2b and 2c, the western boundary current transport is very close to that expected from linear theory (Fig. 1a) which is determined only by the basin width and the wind stress curl. The actual values of  $\nu$  computed at the grid points in Fig. 2c vary from about  $0.2 \times 10^8 \text{ cm}^2 \text{ sec}^{-1}$  throughout most of the open ocean to about  $2.0 \times 10^9 \text{ cm}^2 \text{ sec}^{-1}$  in the western boundary region. This open ocean value is more than an order of magnitude smaller than the constant value which would be necessary in order to avoid the false space oscillation.

The above numerical examples show that the use of nonlinear eddy viscosity permits a lower and more realistic value of eddy viscosity in the open ocean without causing a false computational space oscillation which would occur if a constant viscosity were used. The usefulness of nonlinear eddy viscosity for this purpose is being tested at present in a more general ocean circulation model [21] which is being applied to the problem of predicting large-scale sea surface temperature anomalies in the open ocean as part of NORPAX.

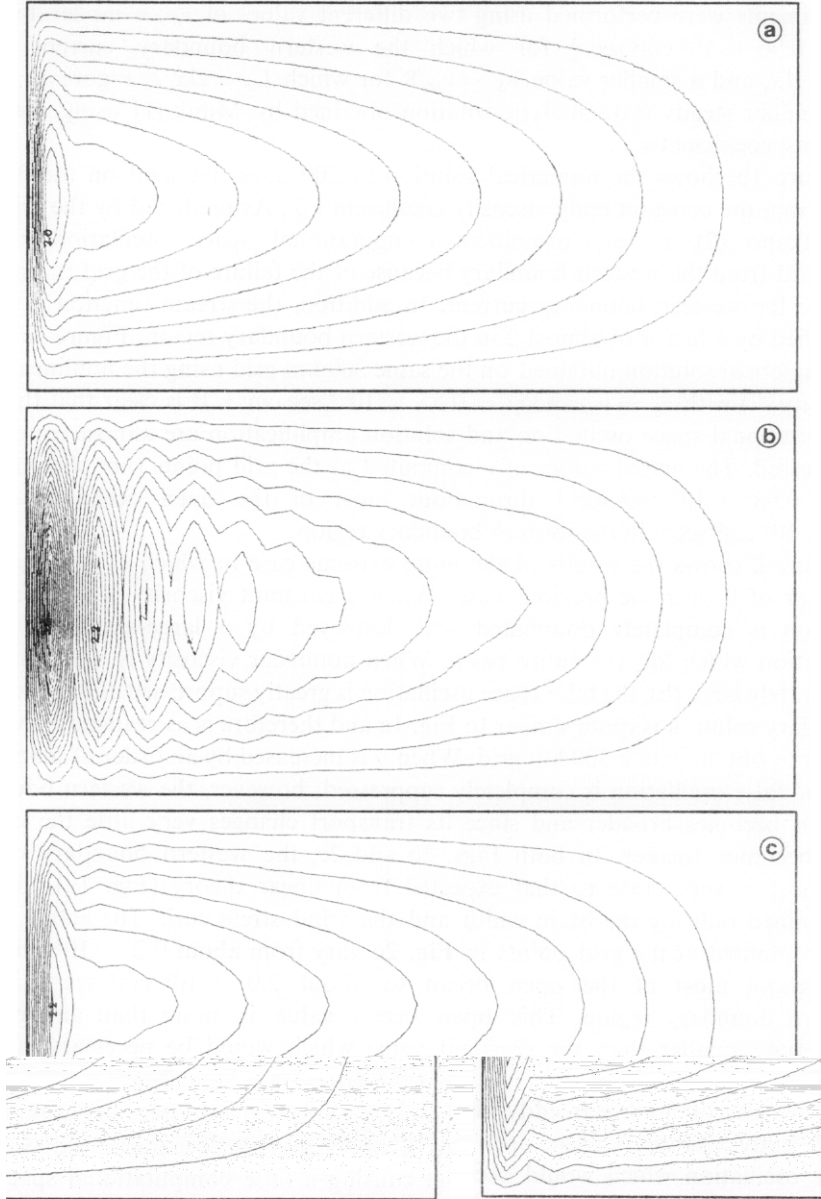


FIG. 1. Stream function solution obtained using the reference viscosity  $\nu_0 = 0.96 \times 10^8 \text{ cm}^2 \text{ sec}^{-1}$ . Solutions are obtained (a) analytically using the constant viscosity  $\nu = \nu_0$ , and numerically using the nonlinear viscosity (7) with (b)  $\gamma = 0$ , (c)  $\gamma = 0.55 \times 10^{-8} \text{ sec cm}^{-2}$ . Isolines of  $\psi$  are drawn for every  $0.2 \times 10^8 \text{ cm}^2 \text{ sec}^{-1}$ .



FIG. 2. Stream function solution obtained numerically using the nonlinear eddy viscosity (7) with  $\nu_0 = 0.12 \times 10^8 \text{ cm}^2 \text{ sec}^{-1}$  and (a)  $\gamma = 0$ , (b)  $\gamma = 5.5 \times 10^{-8} \text{ sec cm}^{-2}$ , (c)  $\gamma = 5.5 \times 10^{-7} \text{ sec cm}^{-2}$ . Isolines of  $\psi$  are drawn for every  $0.2 \times 10^8 \text{ cm}^2 \text{ sec}^{-1}$ .

APPENDIX

The finite difference approximation to (8), (9), and (10) is based upon the placement of variables shown in Fig. 3. The stream function is defined at integer values of the index  $i, j$  while the current is defined at half-integer values. The symbols used to denote spatial derivatives and averages, respectively, over the grid distance  $d$  are

$$\begin{aligned} \delta_x(\ ) &= (1/d)((\ )_{i+1,j} - (\ )_{i,j}), \\ \overline{(\ )}^x &= \frac{1}{2}((\ )_{i+1,j} + (\ )_{i,j}), \end{aligned} \tag{A1}$$

with similar definitions for  $\delta_y(\ )$  and  $\overline{(\ )}^y$ .

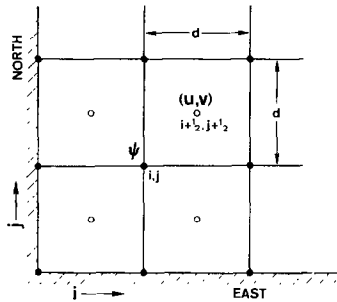


FIG. 3. Placement of the variables in the  $(x, y)$ -plane.

The currents are obtained from the predicted stream function by the following finite difference approximation to Eq. (10).

$$\begin{aligned} v_{i+1/2,j+1/2} &= \delta_x(\overline{\psi}^y), \\ u_{i+1/2,j+1/2} &= -\delta_y(\overline{\psi}^x). \end{aligned} \tag{A2}$$

The eddy viscosity terms, which are also defined at the half-integer points, are given by the following finite difference approximation to (9).

$$\begin{aligned} (F_x)_{i+1/2,j+1/2} &= \delta_x(\overline{\nu}^x \delta_x(u)) + \delta_y(\overline{\nu}^y \delta_y(u)), \\ (F_y)_{i+1/2,j+1/2} &= \delta_x(\overline{\nu}^x \delta_x(v)) + \delta_y(\overline{\nu}^y \delta_y(v)). \end{aligned} \tag{A3}$$

The nonlinear eddy viscosity coefficient  $\nu$  is defined at the half-integer points by the following finite difference approximation to (7).

$$\nu_{i+1/2,j+1/2} = \nu_0 [1 + \gamma((\delta_x(\overline{\xi}^x))^2 + (\delta_y(\overline{\xi}^y))^2)^{1/2} d^3]. \tag{A4}$$



In (A4), the vorticity is defined at the integer-points by

$$\zeta_{i,j} = \delta_x(\bar{v}^y) - \delta_y(\bar{u}^x). \tag{A5}$$

According to the above expressions, the vorticity must be calculated on the lateral boundaries while the velocities and eddy viscosity must be averaged across the boundaries. These quantities are calculated from (A2) using a symmetric profile of  $\psi$  across the boundary (i.e.,  $\partial\psi/\partial n = 0$  on the boundary) as well as  $\psi = 0$  on the boundary itself. This is in accordance with the lateral boundary condition of zero slip (11).

Letting  $( )^n$  denote the time level and  $\Delta t$  the timestep, the finite difference approximation to (8) is

$$\begin{aligned} \frac{\nabla^2(\psi_{i,j}^{n+1} - \psi_{i,j}^{n-1})}{2\Delta t} = & \frac{-\beta}{2d} (\psi_{i+1,j}^n - \psi_{i-1,j}^n) + \left\{ \overline{\delta_x(-\delta_x(\bar{u}^{yy} \bar{v}^x) - \delta_y(\bar{v}^{xx} \bar{v}^y))} \right. \\ & \left. - \overline{\delta_y(-\delta_x(\bar{u}^{yy} \bar{u}^x) - \delta_y(\bar{v}^{xx} \bar{u}^y))} \right\}^n \\ & + \left\{ \delta_x(\bar{F}_y) - \delta_y(\bar{F}_x) \right\}^{n-1} - \frac{F\pi}{\rho DB} \sin\left(\frac{\pi y_j}{B}\right), \end{aligned} \tag{A6}$$

where the finite difference approximation for the Laplacian on the left side of (A6) is the usual five-point approximation

$$\nabla^2\psi_{i,j} = \delta_x\delta_x(\psi) + \delta_y\delta_y(\psi). \tag{A7}$$

Equation (A6) was solved numerically, with  $\psi = 0$  on the boundary, using a fast and accurate cyclic reduction method [17, 18] programmed by Sweet [19]. Time integration was accomplished using a timestep  $\Delta t = 14$  h.

ACKNOWLEDGMENTS

We thank Professor Frank Faulkner of the Naval Postgraduate School and the Environmental Prediction Research Facility for supplying us with the fast Poisson equation solver and for educating us on the method and its use.

This research was sponsored by the National Science Foundation Office of the Decade for Ocean Exploration and the Office of Naval Research as part of the North Pacific Experiment under Office of Naval Research Contract Number N0001475WR50210, through NORPAX.

REFERENCES

1. W. H. MUNK, *J. Meteorol.* **7** (1950), 79.
2. K. BRYAN, S. MANABE, AND R. C. PACANOWSKI, *J. Phys. Oceanog.* **5** (1975), 30.
3. K. TAKANO, *J. Oceanog. Soc. Japan*, in press.

4. K. TAKANO, Y. MINIZ, AND Y. J. HAN, to appear.
5. K. BRYAN AND M. COX, *J. Atmos. Sci.* **25** (1968), 945.
6. K. WYRTKI, *Deep-Sea Res.* **8** (1961), 39.
7. F. WEBSTER, *Tellus* **17** (1965), 239.
8. W. L. GATES, A Note on the Lateral Eddy Viscosity Due to Transient Rossby Waves in a Barotropic Ocean Model, Report RM-6210-ARPA, Rand Corporation, Santa Monica, Calif., 1970.
9. J. SMAGORINSKY, *Monthly Weather Rev.* **91** (1963), 99.
10. C. LEITH, in "Proc. WMO/IUGG Symposium on Numerical Weather Prediction," Tokyo, 1968, p. 140.
11. J. A. T. BYE, *J. Mar. Res.* **28** (1970), 124.
12. W. P. CROWLEY, *J. Computational Phys.* **3** (1968), 111.
13. J. J. O'BRIEN, *Invest. Pesq.* **35** (1971), 331.
14. R. H. KRAICHNAN, *Phys. Fluids* **10** (1967), 1417.
15. C. E. LEITH, *Phys. Fluids* **11** (1968), 671.
16. T. MATSUNO, *J. Meteorol. Soc. Japan* **44** (1966), 76.
17. O. BUNEMAN, A Compact Non-iterative Poisson Solver, Stanford University Institute for Plasma Research, Report 294, 1969.
18. B. BUZBEE, G. GOLUB, AND C. NIELSON, *SIAM J. Numer. Anal.* **7** (1970), 627.
19. R. SWEET, A Direct Method for Solving Poisson's Equation, p. 10, NCAR Report No. 22, National Center for Atmospheric Research, Boulder, Colo. 1972.
20. J. WRIGHT, A Numerical Study of an Idealized Ocean Using Nonlinear Lateral Eddy Viscosity Coefficients, M.S. Thesis, Naval Postgraduate School, 1975.
21. R. HANEY, *J. Phys. Oceanog.* **4** (1974), 145.